



## 1. STM-BJ experiments of 1*H*-imidazole in heavy water (D<sub>2</sub>O)

As discussed in the manuscript, we performed experiments with 1*H*-imidazole in heavy water. Results are shown in Figure S1.

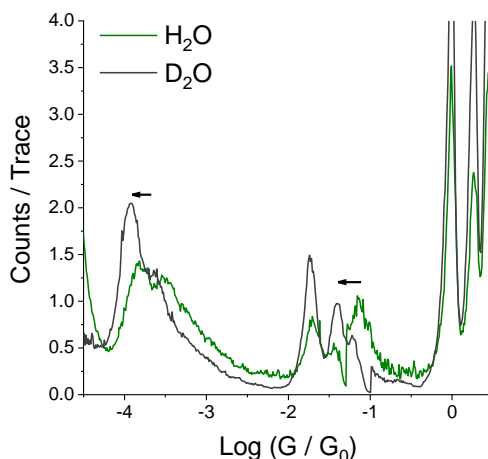


Figure S1: Conductance histogram of 1*H*-imidazole in H<sub>2</sub>O (green) and D<sub>2</sub>O (dark grey)

As can be observed in Figure S1, changing the environment from H<sub>2</sub>O to D<sub>2</sub>O results in a shift of the conductance peaks towards a slightly lower conductance, and different ratio of the various contributions. D<sub>2</sub>O also forms slightly longer junctions, as can be seen by the density maps shown in Figure S2 – the effect could be due to the stronger D<sub>2</sub>O hydrogen bonds, but it is worth pointing out that the observed differences are less than the experimental uncertainties and are not indicative of a clear isotope effect.

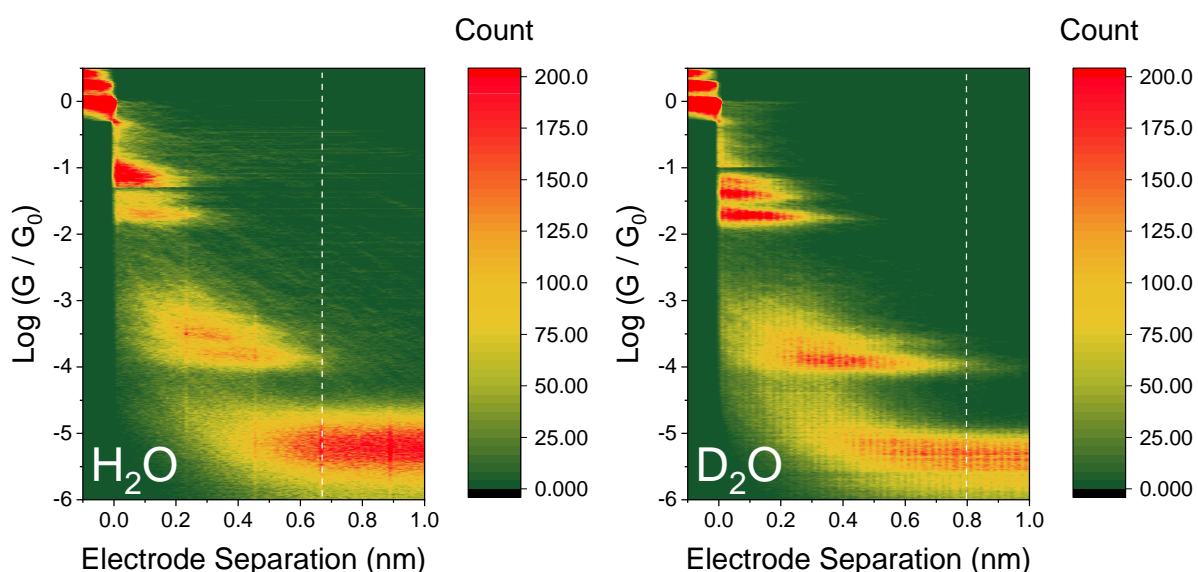


Figure S2: Density map of 1*H*-imidazole in H<sub>2</sub>O (left) and D<sub>2</sub>O (right). Colour scales on the maps are normalised to the number of scan used to compile them (H<sub>2</sub>O: 4210; D<sub>2</sub>O: 4301).

## 2. STM-BJ experiments on Benzimidazole

We also performed the same set of experiments described in the manuscript on benzimidazole, to verify the robustness of the hydrogen bonding chains formed in situ, and to demonstrate that it is indeed mostly NH-N hydrogen bonding responsible for the observed behaviour.

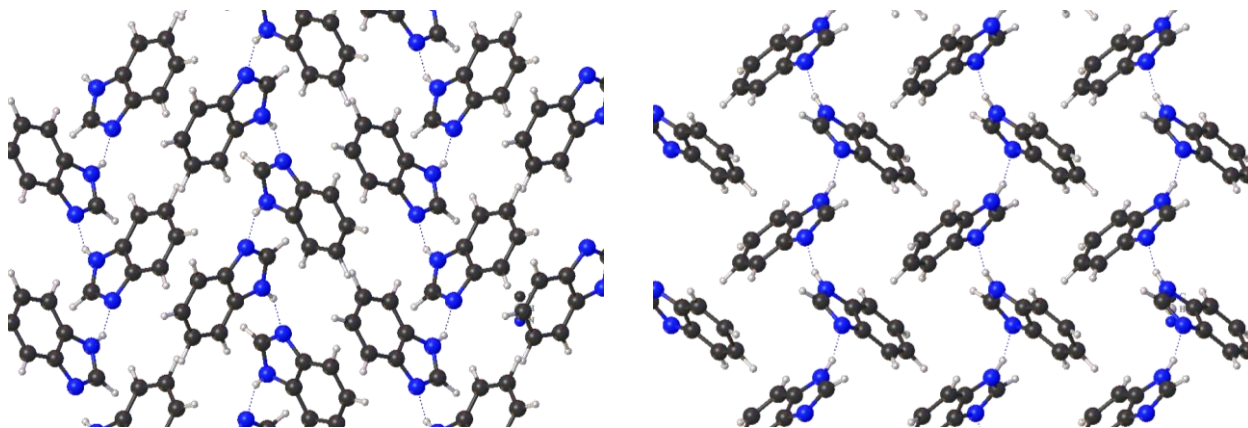


Figure S3: Single-crystal XRD structure of one of the alpha polymorphs of benzimidazole, viewed along the (100) crystallographic plane (left) and along the (001) crystallographic plane (right), to appreciate the H-bonding motif. Structure retrieved from the Cambridge Crystallographic Data Centre, entry BZDMAZ, deposition #1118209.

In a manner similar to 1*H*-imidazole, benzimidazole forms long H-bonded tapes in the solid state, as can be seen in Figure S3.

Measurements of benzimidazole in thoroughly dry conditions, H<sub>2</sub>O or D<sub>2</sub>O gave sets of conductance peaks similar to what has been observed in 1*H*-imidazole, as can be observed in Figure S4-S6.

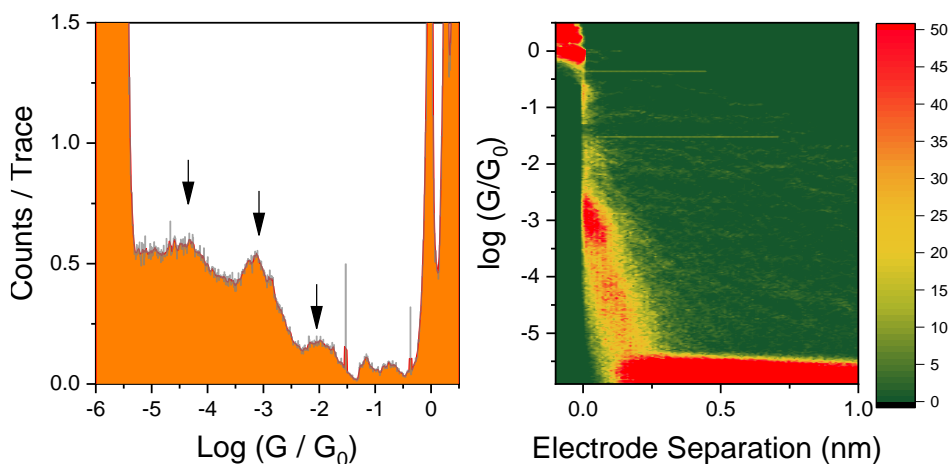


Figure S4: Conductance histogram (left) and 2D density maps for benzimidazole in anhydrous conditions.

## SUPPLEMENTARY INFORMATION

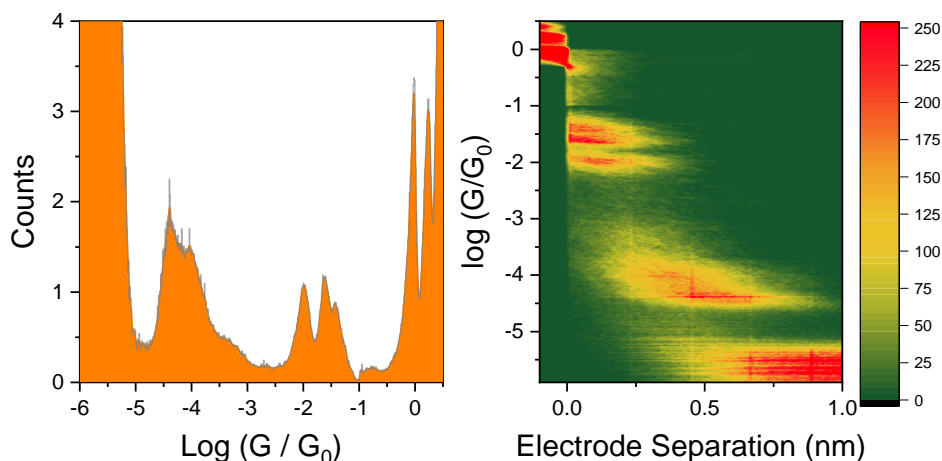


Figure S5: Conductance histogram (left) and 2D density maps for benzimidazole in H<sub>2</sub>O.

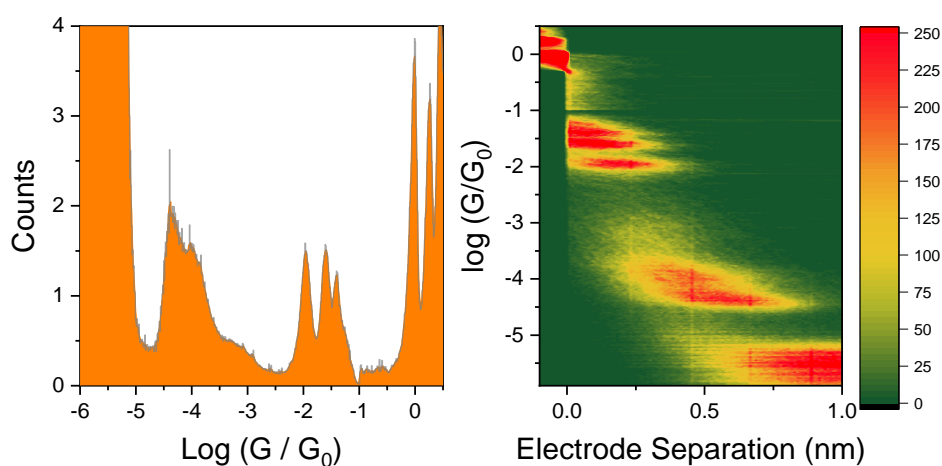


Figure S6: Conductance histogram (left) and 2D density maps for benzimidazole in D<sub>2</sub>O.

With a similar behaviour to 1*H*-imidazole, benzimidazole showed similar conductance values in D<sub>2</sub>O with respect to the measurements in H<sub>2</sub>O.

In addition, we also performed experiments in “wet” solvents, with no effort towards the exclusion of water in commercially available mesitylene and tetrahydrofuran (Figure S7). The main results here is the presence of the peak we attribute to imidazole-H<sub>2</sub>O H-bonding complex in wet environment, appearing as two sharp peaks in the 10<sup>-1</sup> – 10<sup>-2</sup> G<sub>0</sub> region, and the suppression of the conductance peak we attribute to the imidazole H-bonding dimer at 10<sup>-3</sup> G<sub>0</sub>.

## SUPPLEMENTARY INFORMATION

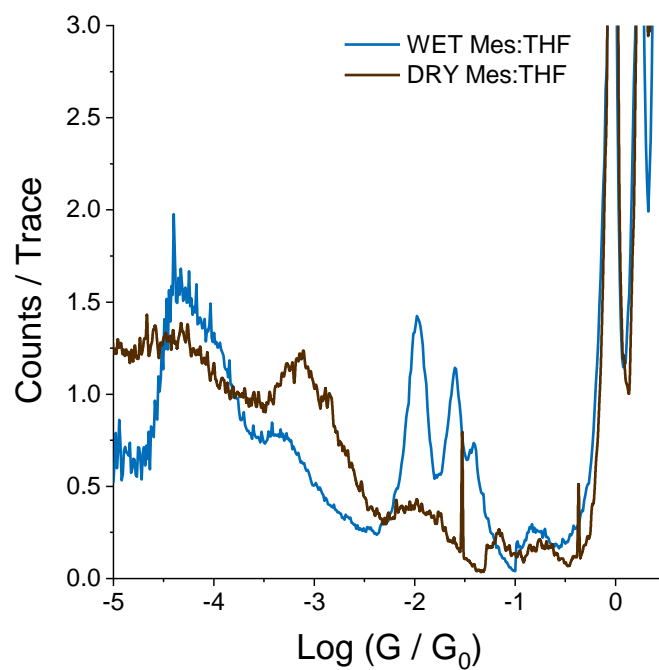


Figure S7: Comparison of conductance histograms of benzimidazole in dry solvents, wet solvents, H<sub>2</sub>O and D<sub>2</sub>O

---

The overall results therefore strengthen our claim of a strong influence of the environment (in this case, H-bonding environment) on the conductance behaviour of imidazolic compounds.

## 3. DFT Calculation for the benzimidazole series

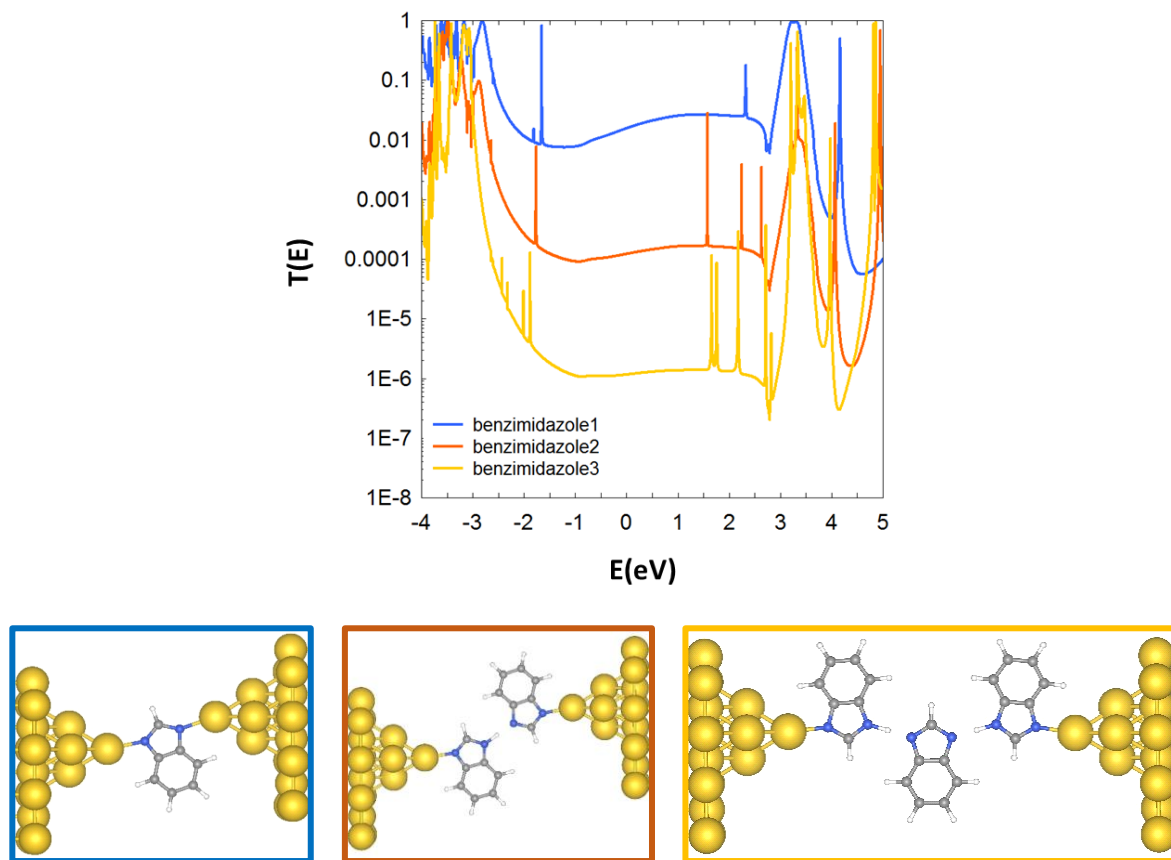


Figure S8: DFT transmission coefficient vs energy for the benzimidazole series (top) and colour-coded DFT-optimised structures used for the calculations (bottom).

Figure S8 shows the transmission coefficient of benzimidazole series. Like the imidazole series, the conductance of benzimidazole drops by about 2 orders of magnitude upon adding each H-bonding benzimidazole to the junction. Furthermore, the trend from our calculations is in good agreement with experimental result.

## 4. DFT calculations for protonated junctions

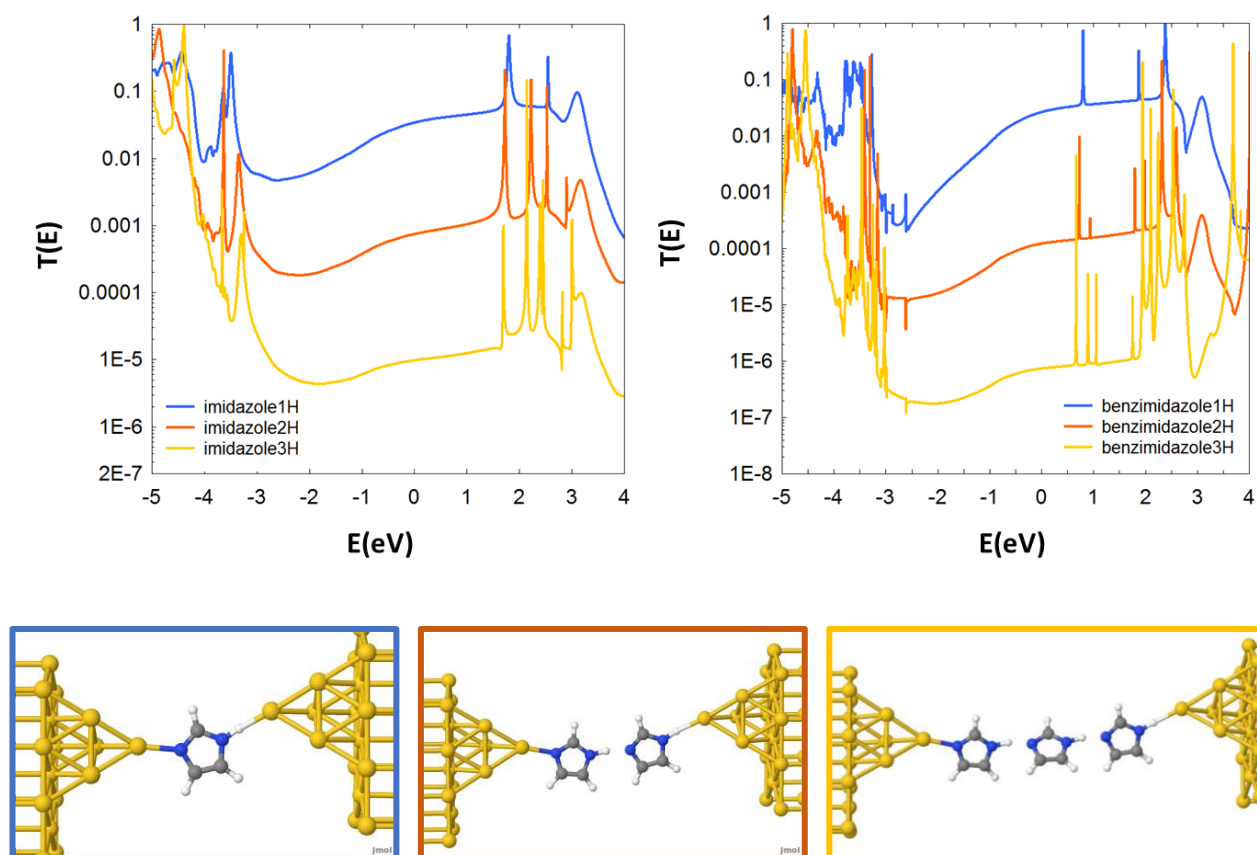


Figure S9: Transmission coefficient vs energy for protonated imidazole (top left) and benzimidazole (top right). Colour-coded illustrative structures for the imidazole series used for the above calculations shown in the bottom panel.

Figure S9 shows the transmission coefficient of the protonated imidazole and benzimidazole series. Similar to the result shown for non-protonated junctions in Figure 4 of the main paper and Figure S8, increasing the number of H-bonded units bridging the two electrodes reduces the conductance of the system. The overall conductance values are slightly lower than non-protonated series, as a result of a reduced electrode-molecule coupling.

## 5. Additional calculations in the presence of water

In addition to the structures presented in the main paper in Figure 4b, we performed calculations on other possible conformers of the junctions in the presence of water, either with water adsorbed at an electrode or with different motifs of H-bonding.

The overall results help in understanding the peak splitting observed, for instance, in Figure 2b of the main paper. Subtle differences in the junction structure result in different transmission coefficient, and therefore, slightly different conductance values at the Fermi level of Au.

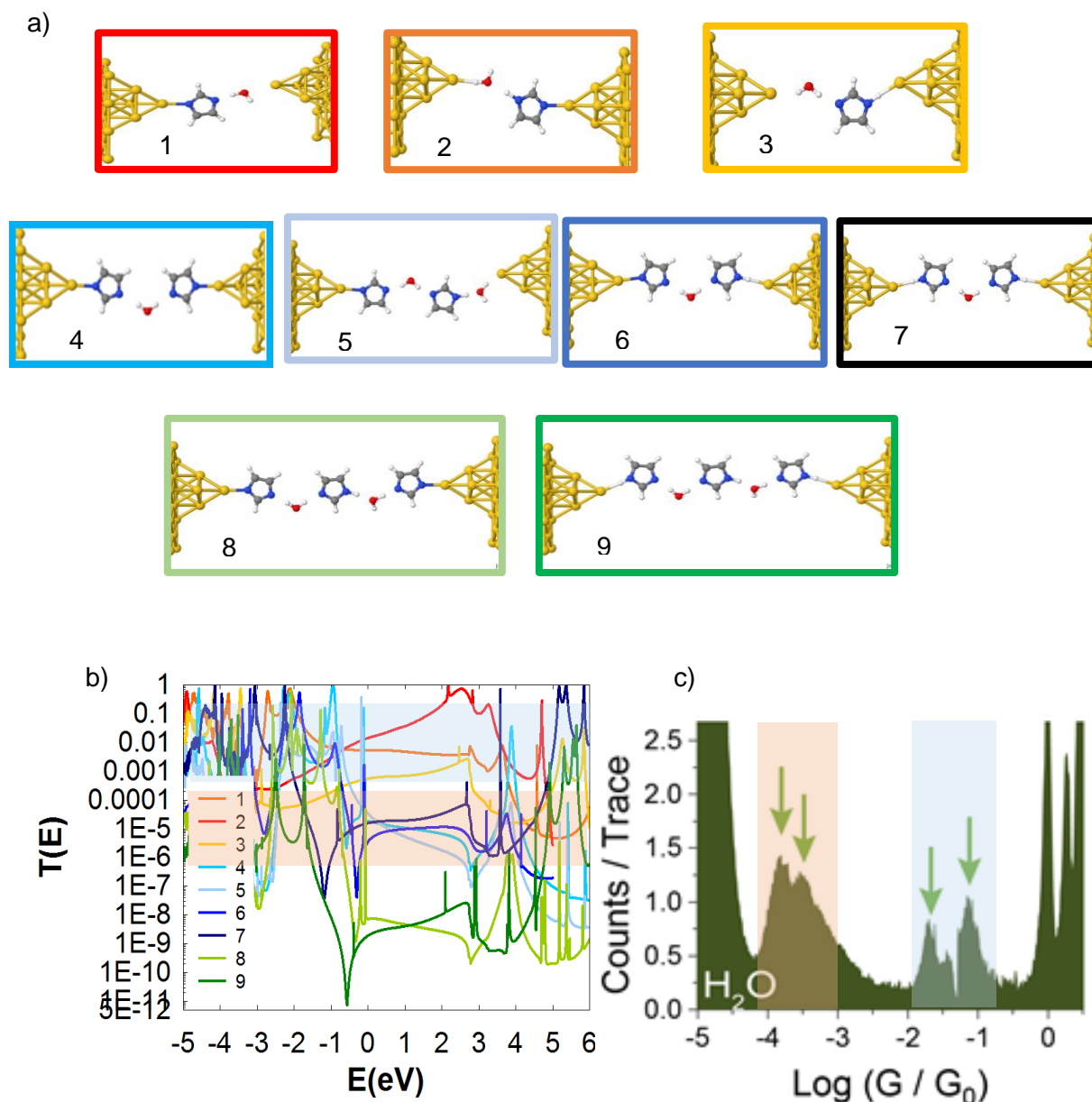


Figure S10: a) Colour-coded examples (1-9) of relaxed geometries and b) transmission coefficient vs energy plot for the imidazole series in the presence of water, with different relaxed conformations adopted in the junctions c) experimental measurement of the imidazole series in presence of water. The highlighted area in b and c shows comparison between theory and experimental data.



## SUPPLEMENTARY INFORMATION

As shown in Figure S10, the transmission coefficients of junctions with three imidazoles suggest that the conductances of these are too low to be measured experimentally. The transmission coefficients of the other junctions suggest that the conductances of the single-imidazole junctions (1, 2 and 3 Figure S10b) should be two orders of magnitude higher than those of junctions with two imidazoles (4-7 Figure S10b). Therefore, we identify the experimental peaks around  $\text{Log } G/G_0 = -1$  to  $-2$  with single imidazole junctions and those around  $\text{Log } G/G_0 = -3.5$  to  $-4$  with two-imidazole junctions.

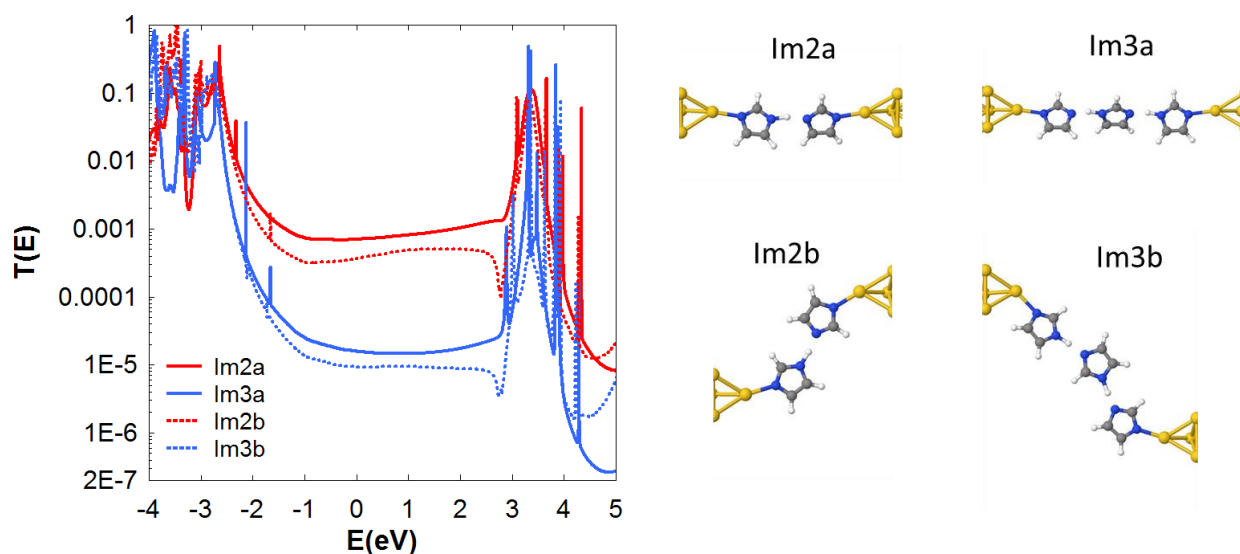
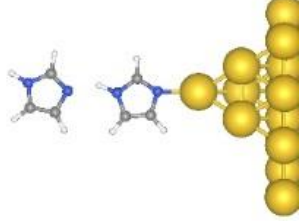
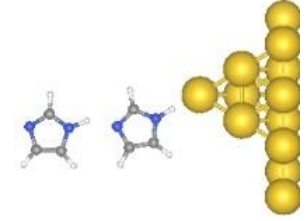
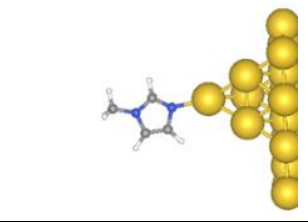
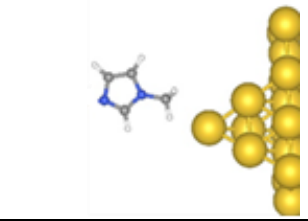
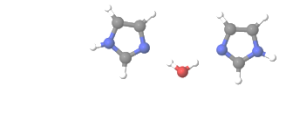


Figure S11: Transmission coefficients of imidazole structures with either 2 (red) or 3 (blue) imidazole units, each for two different H-bonding orientation (left) and corresponding relaxed structures (right).

## 6. Binding Energy Calculations

Table S1. Binding energy calculation

| $\Delta E$ | Structure   | Notes  |
|------------|---|--|
| -0.623 eV  |    | Imidazole<br>Deprotonated Junction                         |
| -0.347 eV  |    | Imidazole<br>Protonated Junction                           |
| -0.444 eV  |   | 1-methylimidazole<br>N lone pair interaction               |
| 0.051 eV   |  | 1-methylimidazole<br>N(CH <sub>3</sub> ) – Au interactions |
| -0.786 eV  |  | H-bonding through water                                    |

## 7. Molecular Junction Lengths

Table S2. Calculated vs. measured molecular junction length

| Molecule                  | Molecular distance (nm) (protonated) | Au-Au distance (nm) (protonated) | Molecular distance (nm) (deprotonated) | Au-Au distance (nm) (deprotonated) | Experimental break off distances |
|---------------------------|--------------------------------------|----------------------------------|--|------------------------------------|----------------------------------|
| Imidazole 1               | 0.32                                 | 0.72                             | 0.22                                   | 0.67                               | 0.69                             |
| Imidazole 2               | 0.79                                 | 1.2                              | 0.72                                   | 1.17                               | 0.86                             |
| Imidazole 3               | 1.28                                 | 1.68                             | 1.18                                   | 1.63                               | 1.06                             |
| Benzimidazole1            | 0.32                                 | 0.75                             | 0.23                                   | 0.71                               | 0.67                             |
| Benzimidazole2            | 0.81                                 | 1.25                             | 0.72                                   | 1.16                               | 0.77                             |
| Benzimidazole3            | 1.22                                 | 1.70                             | 1.18                                   | 1.63                               | 0.91                             |
| All Imidazole series +H2O |                                      |                                  |  |                                    |                                  |
| imi2+H2O                  | —                                    | —                                | 0.94                                   | 1.38                               | 0.81                             |
| imi1+H2O_1                | —                                    | —                                | 0.49                                   | 0.99                               | 0.82                             |
| imi1+H2O_2                | —                                    | —                                | 0.53                                   | 1.04                               | 1.13                             |
| imi2+2H2O                 | —                                    | —                                | 1.21                                   | 1.60                               | 1.22                             |
| imi3+H2O                  | —                                    | —                                | 1.63                                   | 2.06                               | —                                |
| imi1H+H2O                 | 0.55                                 | 1.02                             | —                                      | —                                  | —                                |
| imi2H+H2O_1               | 0.99                                 | 1.41                             | —                                      | —                                  | —                                |
| imi2H+H2O_2               | 1.09                                 | 1.48                             | —                                      | —                                  | —                                |
| imi3H+H2O                 | 1.76                                 | 2.13                             | —                                      | —                                  | —                                |

The theoretical break-off distance is the linear gold-to-gold distance, while the structures may be staggered as shown in Figure S11 for Im2b and Im3b. This would account for the longer theoretical values. However, the key point here is that experimental break-off distances values can only be accounted for by the oligomeric structures.

SUPPLEMENTARY INFORMATION

8. Molecular Orbitals

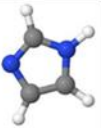
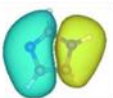

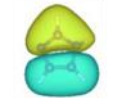

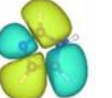
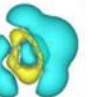
|   | HOMO-2  | HOMO-1  | HOMO  | LUMO   | LUMO+1  | LUMO+2  |
|---|---|---|---|--|---|---|
|  |  |  |  |  |  |  |
| $E_f = -1.2092$ eV  | -6.15918 eV   | -5.25102 eV   | -4.88527 eV   | 0.37644 eV   | 1.42817 eV  | 2.18874 eV  |

Figure S12: DFT based orbital diagrams for imidazole

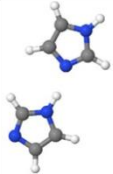

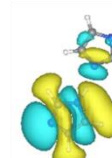
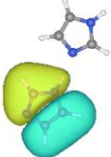
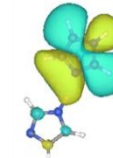
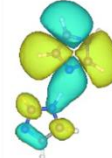
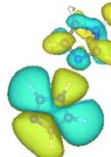
|   | HOMO-2  | HOMO-1  | HOMO  | LUMO   | LUMO+1  | LUMO+2  |
|---|---|---|---|--|---|---|
|  |  |  |  |  |  |  |
| $E_f = -2.8321$ eV  | -5.20298 eV   | -4.42628 eV   | -4.01114 eV   | -0.53457 eV  | 0.40400 eV  | 1.35697 eV  |

Figure S13: DFT based orbital diagrams for imidazole H-bonded dimer.

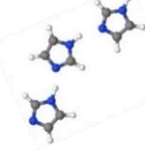
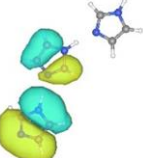
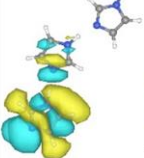
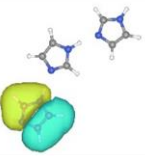
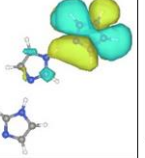
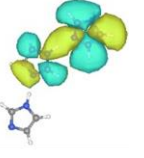
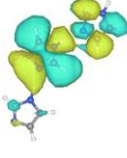
|   | HOMO-2  | HOMO-1  | HOMO  | LUMO   | LUMO+1  | LUMO+2  |
|---|---|---|---|--|---|---|
|  |  |  |  |  |  |  |
| $E_f = -3.0107$ eV  | -4.85362 eV   | -4.11535 eV   | -3.67902 eV   | -0.87942 eV  | 0.03147 eV  | 0.45139 eV  |

Figure S104: DFT based orbital diagrams for imidazole H-bonded trimer.

SUPPLEMENTARY INFORMATION

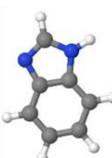
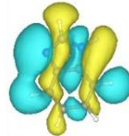
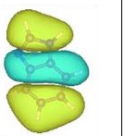
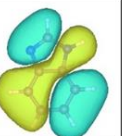
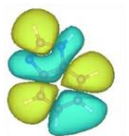
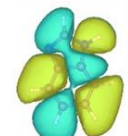
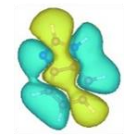
|   | HOMO-2  | HOMO-1  | HOMO  | LUMO   | LUMO+1  | LUMO+2  |
|---|---|---|---|--|---|---|
|  |  |  |  |  |  |  |
| $E_f = -2.5682$ eV  | -5.47339 eV   | -5.08005 eV   | -4.96157 eV   | -0.80440 eV  | 0.15990 eV  | 0.96143 eV  |

Figure S115: DFT based orbital diagrams for benzimidazole


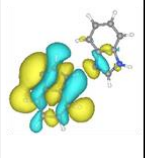
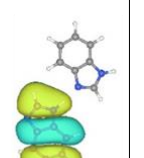
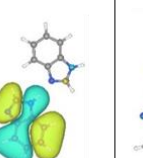
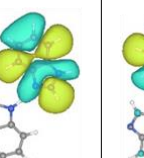
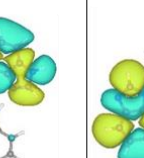
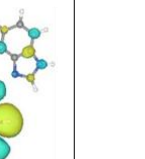
|   | HOMO-2  | HOMO-1  | HOMO  | LUMO   | LUMO+1  | LUMO+2  |
|---|---|---|---|--|---|---|
|  |  |  |  |  |  |  |
| $E_f = -3.0498$ eV  | -4.85005 eV   | -4.47643 eV   | -4.35313 eV   | -1.53179 eV  | -0.49739 eV   | -0.23391 eV   |

Figure S126: DFT based orbital diagrams for benzimidazole H-bonded dimer.

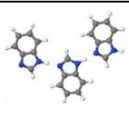
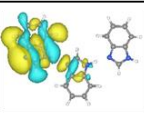
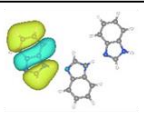
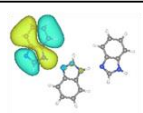
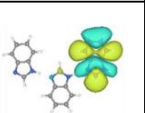
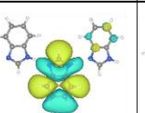
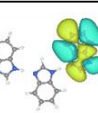
|   | HOMO-2  | HOMO-1  | HOMO  | LUMO   | LUMO+1  | LUMO+2  |
|---|---|---|---|--|---|---|
|  |  |  |  |  |  |  |
| $E_f = -3.1571$ eV  | -4.59714 eV   | -4.23972 eV   | -4.11400 eV   | -1.82330 eV  | -0.96325 eV   | -0.76684 eV   |

Figure S 137: DFT based orbital diagrams for benzimidazole H-bonded trimer.